Available online at www.sciencedirect.com
ScienceDirect
Cement and Concrete Research 37 (2007) 1613–1623
Cement and Concrete Research

Quantitative analysis of the microstructure of interfaces in steel reinforced concrete

A.T. Horne [a,b], I.G. Richardson [a,*], R.M.D. Brydson [b]

[a] School of Civil Engineering, University of Leeds, Leeds, LS2 9JT, United Kingdom
[b] Institute for Materials Research, University of Leeds, Leeds, LS2 9JT, United Kingdom

Received 25 October 2006; accepted 19 August 2007

Abstract

This article reports the results of a backscattered electron imaging study of the microstructure of the steel– and aggregate–cement paste interfaces in concrete containing 9 mm ribbed reinforcing bars. The water to cement (*w*/*c*) ratio, hydration age, steel orientation, and surface finish were varied. For vertically cast bars, there was more calcium hydroxide (CH) and porosity and less unreacted cement at both the steel– and aggregate–cement paste interfaces when compared to the bulk cement paste. As the hydration age increased, the porosity near the interfaces decreased, and the CH increased with more CH close to the steel than to the aggregate. Horizontal bars had more porosity and less CH under them than above. An increase in the *w*/*c* ratio produced interfaces of higher porosity and lower levels of CH. Wire-brush cleaned bars had higher levels of CH at the steel–cement paste interface at 365 days when compared to uncleaned bars.

Keywords: Backscattered electron imaging (B); Interfacial transition zone (B); Steel reinforced concrete; Image analysis (B); $Ca(OH)_2$ (D)

1. Introduction

Steel cast within reinforced concrete is normally protected from corrosion by a very thin insoluble oxide layer that forms on its surface because of the high pH of the pore solution [1]. Any effect that results in the disruption of this layer – for example, a reduction in the pH caused by carbonation of the cement paste – would lead to corrosion of the steel, which can lead to costly repairs, or at worst failure [2]. It is therefore essential that the high pH be maintained, particularly in the region close to the steel. Understandably, given the importance of steel reinforced concrete structures to the Built Environment, there have been many attempts to characterize the steel–cement paste interface region using various microscopy techniques. The most commonly adopted has been secondary electron imaging of fracture surfaces [e.g. [3–5]], no doubt because specimens are very easily prepared for examination. These studies generally concluded that the interface is largely composed of calcium hydroxide (CH), and that there is therefore a larger amount of CH present at the steel–cement paste interface than in the bulk cement paste. This has led to the belief that the local pH buffering capacity in the interface region is enhanced by extra CH, which consequently results in the steel being protected by an oxide layer for longer periods of time than otherwise [3], which would of course very desirable. The explanation proposed to account for an enhanced quantity of CH at the interface is that shortly after casting the concrete, the reinforcing bars are surrounded by a large amount of water, which provide large areas into which Ca^{2+} ions can diffuse from outside the interface region, resulting in the formation of regions enriched in CH [6]. Unfortunately, it is difficult to assess the correctness of this rather desirable scenario because of the limitations of secondary electron imaging of fracture surfaces: i.e. unrepresentative sampling (because the fracture passes through the weakest path), issues concerning user bias, and that any carbonation of the fracture surfaces subsequent to fracture would result in the formation of calcium carbonate, which can be mistaken for CH. It should be noted that the existence of a layer of CH at the interface has been disputed in a number of papers [7–10],

* Corresponding author. Tel.: +44 113 343 2331; fax: +44 113 343 2265.
E-mail address: I.G.Richardson@leeds.ac.uk (I.G. Richardson).

0008-8846/$ - see front matter © 2007 Elsevier Ltd. All rights reserved.
doi:10.1016/j.cemconres.2007.08.026

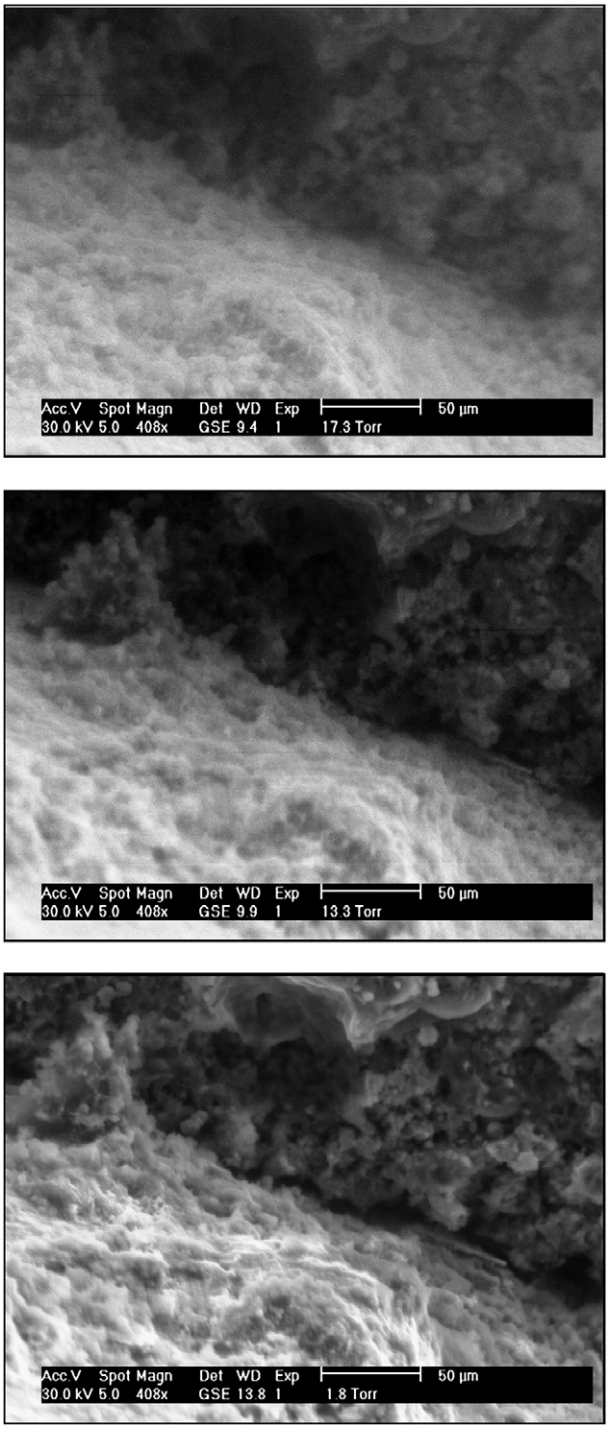

Fig. 1. Secondary electron images of a concrete–steel interface obtained in an ESEM at three relative humidities. The steel is in the bottom half of the micrographs. The relative humidity (RH) decreases from top to bottom, from 100% to approximately 95% to approximately 15%. The size of the gap at the interface increases with decreasing RH.

although the relevance of the results in two of them [7,8] to steel reinforced concrete must be open to question because the steel in the specimens was too small to adequately simulate the interface in a real system. Clearly the existence or otherwise of an enhanced quantity of CH at the interface is important because of the consequences for the durability of steel reinforced structures. Quantifying the amount of CH at the interface has not however, proved to be straightforward. The backscattered electron (BSE) imaging study reported by Zayed [9,10] did involve real steel reinforcing bars (rebar) but only 16 images were collected for each sample and the analysis involved transverse sections of vertically cast rebar, both of which limit the significance of the results (as discussed later). Aside from Zayed's study, there appears to have been no other quantitative study of the microstructure of the concrete–steel interface using BSE imaging, presumably because of the extreme differences in hardness across the interface, which makes polishing problematic. It was found in the current work that it is possible to produce specimens that are sufficiently flat across the steel–cement paste interface for BSE imaging, but only after a lengthy process of optimization of the polishing procedure. Quantitative results are reported in this article for steel reinforced concretes made with two different *w*/*c* ratios at four different curing times, for wire-brushed or uncleaned surfaces, and for interfaces with a vertically or horizontally oriented rebar.

2. Experimental procedure

A 9 mm ribbed reinforcing steel was cast vertically and horizontally in concrete containing ordinary Portland cement; the rust and mill scale that was on the bars was left for most experiments so as to be as realistic as possible. A mix design of 3:2:1 coarse aggregate: fine aggregate: cement was chosen, with *w*/*c* ratios of 0.49 or 0.7, which had 28-day compressive strengths of 61 and 36 MPa respectively. The coarse aggregate was a quartz river gravel (< 14 mm) and the fine aggregate was a quartzitic sand. Samples were cured in a fog room at 20 ± 2 °C. Cores, with the reinforcing bars central, were extracted from the concrete at 4 ages: 1, 7, 28 and 365 days. The cores were sectioned along the bar for parallel analysis, or across the bar for transverse analysis. When cutting the cores for transverse analysis it was not possible to know the position of the cut surface in relation to the ribs, which reduces the applicability of the results because the interface would be different at various positions around the ribs (as demonstrated in Section 3). Parallel-cut sections were thus used for all quantitative analysis; the rib areas could therefore be avoided, a problem that was not addressed in the papers by Zayed [9,10] which will have undoubtedly compromised the results.

The sections were freeze-dried and then impregnated with epoxy resin (Epofix Kit, Struers, Glasgow, UK) under vacuum and, after hardening, polished to a flat surface on a rotary grinding/polishing machine (PdM-Force20 mounted on Struers Rotopol-35), using silicon carbide paper of different grades. The samples were subsequently polished with diamond paste; the process was kept as short as possible in order to minimize the effects of preferential polishing at the steel–cement paste interface. This procedure meant that it was not possible to remove the larger scratches and holes, which were therefore avoided during analysis. The surface of the polished samples was carbon coated in a vacuum coating unit (EMSCOPE TB500, U.K.). When viewing the samples in the scanning electron microscope (SEM)

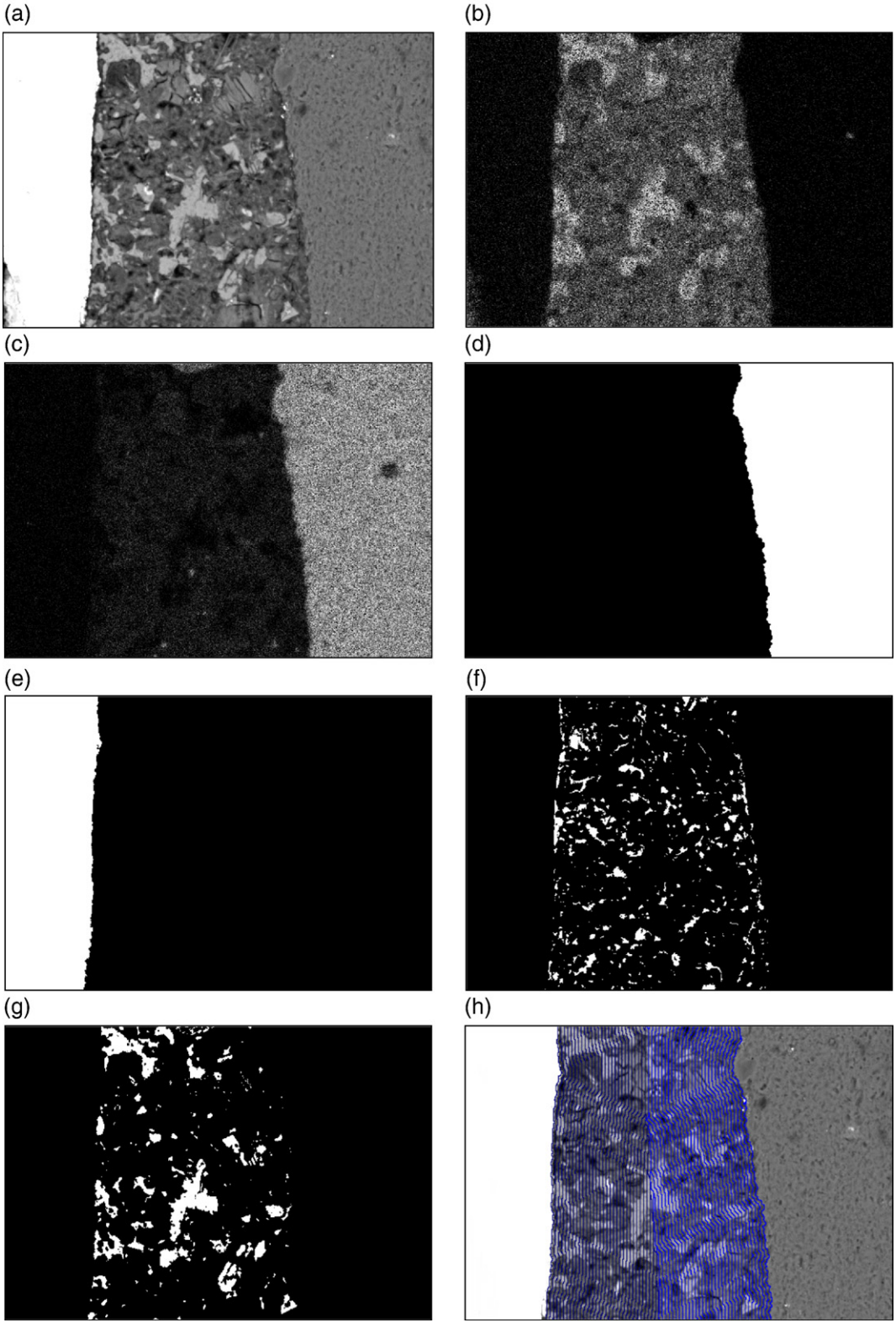

Fig. 2. Illustration of the procedure used to produce the phase-distribution profiles using a typical BSE image of a region in a 0.49 *w/c* ratio concrete that has both steel– and aggregate–cement paste interfaces (a). The steel is white and can be seen in the left part of the micrograph; in this case there is no shrinkage gap along the interface. (b) to (h) illustrate the procedure used for the quantitative analysis of the image. The aggregate–paste interface was identified using the ratio of the Ca (b) and Si (c) X-ray dot maps collected at the same time as the BSE image, which were used to produce a binary mask representing the aggregate (d); a binary mask for steel (e) was easily produced because of the big difference in the backscattering coefficient of the steel and the rest of the microstructure (i.e. it appears white on the images); and binary masks for the porosity (f), unreacted cement and calcium hydroxide (g) were produced from the grey-scale histograms (after removal of the contributions from steel and aggregate), as described in Scrivener et al. [13]. The strips that were progressively grown perpendicular to the steel– or aggregate–cement paste interfaces are illustrated in (h); the strips are 1.86 μm wide and were grown up to a total distance of 120 μm unless prevented from extending so far by the presence of aggregate–cement paste interfacial regions, as in this particular image. The width of the micrograph is 240 μm.

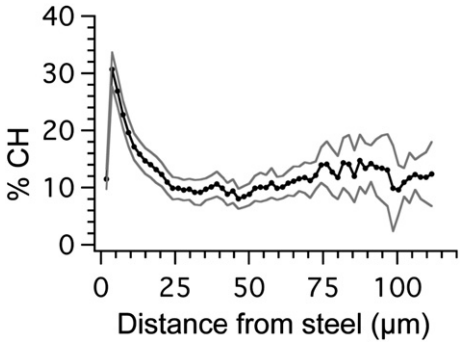

Fig. 3. A typical example of the results of the image analysis procedure (for vertically cast steel at 28 days in a concrete with a *w/c* ratio of 0.49), which shows the mean percentage of calcium hydroxide with distance from the steel–cement paste interface. The grey lines indicate 95% confidence intervals (i.e.± $t_{(n-1,0.025)}\times(s/\sqrt{n})$), which get larger as the number of images contributing to the calculation reduces at greater distances from the interface.

in BSE imaging mode a very thin dark line was often observed around the steel. Freshly fractured surfaces of reinforced concrete were dried within an environmental SEM (Philips XL-30 operated at 30 kV) in order to check whether the dark line was an artefact of drying. It was observed that as the vacuum in the ESEM was increased, the sample dried and the paste shrank away from the steel, as illustrated in Fig. 1. The width of the shrinkage crack varied between interfaces, from zero to a maximum of about 3 μm, although it was usually much narrower than this upper value. Whilst it was not possible to avoid the formation of the crack, the knowledge that it had formed in this way meant that it could be ignored during image analysis; the interface was taken to be at the paste side of the crack and so pixels corresponding to the crack in the images are not included in the values for porosity.

The polished samples were examined using a CamScan Series 4 SEM (operated at 20 kV and a working distance of 28 mm) equipped with an Oxford Instruments' energy dispersive X-ray (EDX) detector with associated image capture software (Link Isis) for the recording of the X-ray maps and BSE images, which for quantitative analysis were taken at 500×. The method adopted for analysis was similar to that used by Head [11] (and outlined by Richardson [12]) where analysis regions are progressively extended from interfaces using an image analysis package (KS400 from Imaging Associates Ltd.); phase quantifications could thus be established at various distances from the interface. The area fractions of CH, porosity (>0.5 μm), and unreacted cement could all be segmented on the basis of average atomic number contrast [13] and displayed as a percentage of the total area; the sum of these subtracted from 100% is presented in the results as 'undesignated product', but is largely calcium silicate hydrate (C–S–H), which in some areas is intermixed with small amounts of CH and calcium sulpho-aluminate hydrate phases on a scale too fine to be resolved by BSE imaging. The procedure is illustrated in Fig. 2. A total of up to 60 images were taken at each age for each system. This was generally obtained from 2 different samples, with up to 30 images recorded from each. This was the highest practicable number possible within reasonable timescales and was sufficient to provide a statistically significant profile of the concrete–steel interfacial zone. It is important to remember that whilst the area fraction of phases in hardened cement pastes determined by image analysis of 2D sections is directly equivalent to the volume fraction, it is not possible to measure other 3D information such as size distributions or phase connectivity

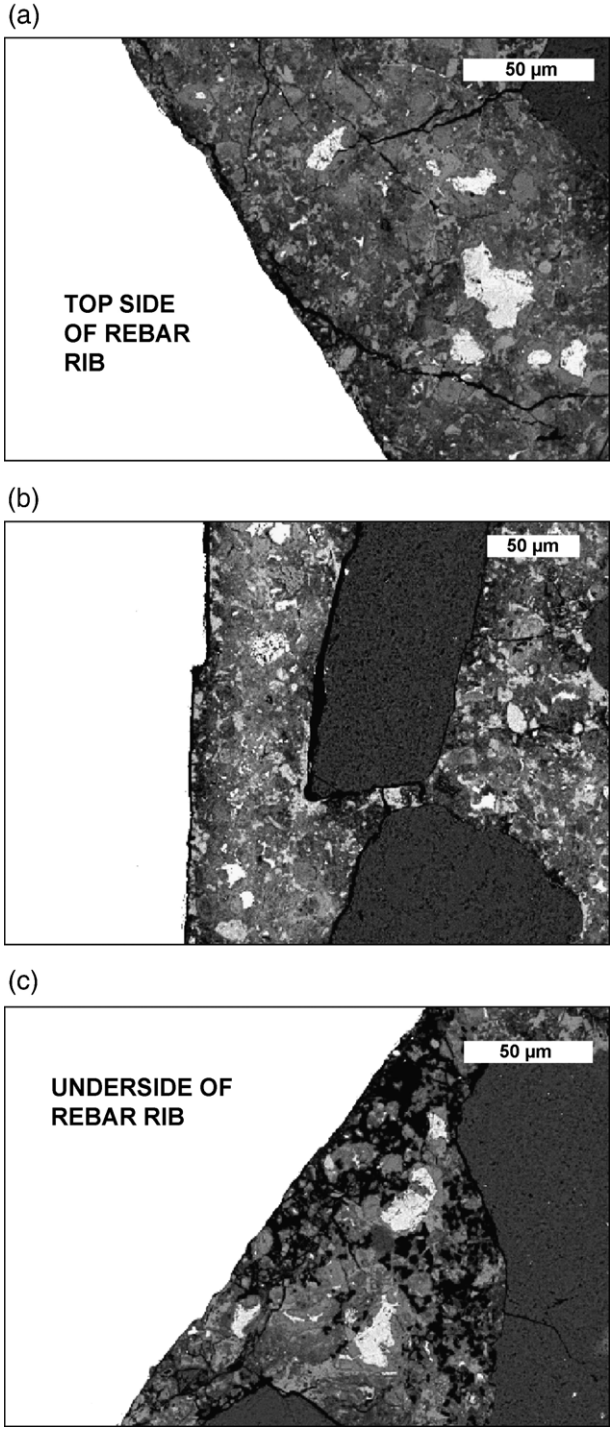

Fig. 4. Backscattered electron images illustrating the variable microstructure found around the ribs on vertically cast rebar, including the topside of a rib (a), the middle (b), and the underside (c).

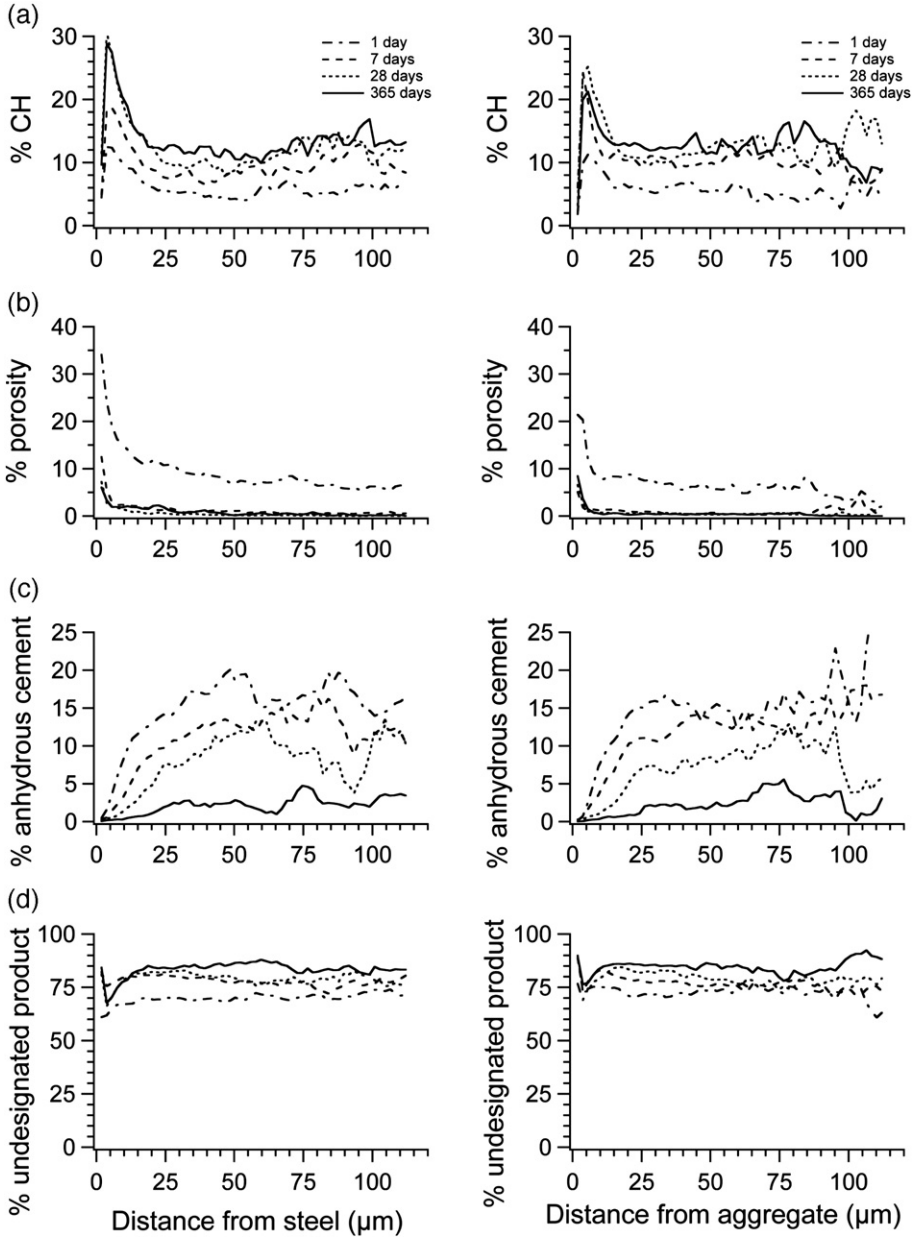

Fig. 5. Microstructural gradients in the interfacial region between cement paste and vertically cast steel (left) and aggregate (right) at four ages in a concrete with a *w/c* ratio of 0.49: (a) calcium hydroxide, (b) porosity, (c) unreacted clinker phases, and (d) undesignated hydration products (mainly C–S–H).

[14]; so, for example, whilst the fraction of pores was measured in this work, the 3D connectivity of those pores – which is important for transport properties – could not be determined. The *w/c* ratio was varied (0.49 and 0.70), the surface of the bar was either in the as-received state (i.e. with mill scale and a moderate amount of rust) or wire-brush cleaned, and the orientation of the bar was also varied (i.e. either vertical or horizontal). The regions for image analysis were ≈170 μm in length (parallel to the interface) and were progressively grown perpendicular to the interface in 1.86-micrometre strips to a total distance of 120 μm from the steel interface; each strip was averaged across all the images with the statistics becoming less good at greater distances from the interface because of a reduction of the number of images used in the calculation due to the presence of aggregate particles (and so aggregate–cement paste interfacial regions), which is well illustrated by the example in Fig. 2. The total length of steel–cement paste interface sampled for each specimen was therefore approximately 1 cm. A typical example of the results of the image analysis procedure is shown in Fig. 3.

3. Results and discussion

3.1. System with w/c = 0.49 and a vertical bar with mill scale/rust

Qualitative analysis of the samples indicated that there was a build up of CH along the steel interface; it was not however a

continuous layer. The concrete under the rebar ribs was very poor quality: the collection of bleed-water had created areas that could not be filled with hydration products, in some systems up to 365 days, which is illustrated in Fig. 4. This is the reason why all quantitative measurements were made using sections cut along the length of the rebar.

Fig. 5 shows the phase-distribution profiles from the steel– and aggregate–cement paste interfaces for the system with the lowest *w/c* ratio (0.49); the rebar was cast vertically and was in the as-received state (i.e. with mill scale and a moderate amount of rust).

At all ages there is a greater concentration of CH close to the steel bar compared with the bulk paste (for example at 365 days, there is 30% CH close to the steel and around 12% in the bulk paste). At no distance is there a continuous layer of CH. At 1 day there is a very large amount of porosity (>30%) at the steel–cement paste interface and around 8% in the bulk paste. By 7 days there is still significant porosity very close (within a few μm) to the steel but very few pores (>0.5 μm) in the bulk paste. The interface does change after 7 days with CH still being formed up to 28 days. Reduced levels of anhydrous cement are found at the interface, which is expected due to the so-called 'wall' effect (which has been discussed widely in the literature with reference to the interfacial transition zone around aggregate particles, for example Scrivener et al. [15]). The extra CH close to the interface is offset largely by a reduced amount of undesignated product (which is largely C–S–H). The aggregate and steel profiles are observed to be very similar, but with a lower concentration of CH very close to the aggregate interface than to the steel.

3.2. Effect of varying w/c ratio

Vertical, uncleaned bars were also cast into samples with a higher *w/c* ratio (0.70); the phase-distribution profiles from the steel–cement paste interfaces are shown in Fig. 6. There is a reduction (from 30 to 20%) in the maximum amount of CH close to the interface as the *w/c* ratio increases from 0.49 to 0.7. There is a much higher level of porosity up to 28 days with the 0.7 *w/c* ratio concrete than with the 0.49, but all systems have very few pores (>0.5 μm) by 365 days.

3.3. Effect of bar orientation

A similar uncleaned ribbed reinforcing bar was cast horizontally in a 0.49 *w/c* ratio concrete. Phase-distribution profiles within the concrete were measured from both the top and bottom of the bar; the results are shown in Fig. 7. The top of the bar (Fig. 7, left) displays similar profiles to the vertical bar of the same *w/c* ratio (Fig. 5), although the degree of reaction is generally lower (and there is therefore less CH in the bulk paste), which is presumably due to the reduced availability of water. The bottom of the bar (Fig. 7, right) shows an interfacial microstructure that is completely different from the others, with the phase-distribution profiles affected dramatically by the bleed-water zone. There is no build up of CH underneath the bar because the very large water-filled pores are much too large and distant from hydrating cement particles to be filled with hydration products. The dramatic difference in interfaces between the top and bottom of the bars is evident in the SEM BSE micrograph shown in Fig. 8. Beyond the bleed-water zone, the microstructure of the bulk cement paste is similar to the top of the bar except that at there is generally a greater degree of reaction and consequently more CH.

Interfaces were also examined for uncleaned ribbed reinforcing bars cast horizontally in a 0.7 *w/c* ratio concrete. Phase distributions were again calculated for both the top and bottom of the bar, as shown in Fig. 9. The tops of the bars exhibit a

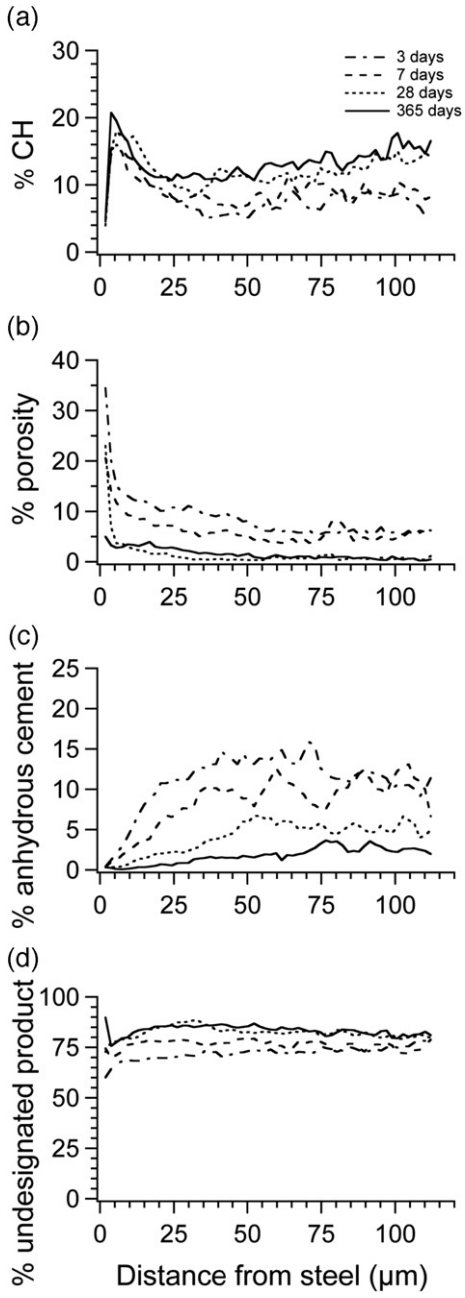

Fig. 6. Microstructural gradients in the interfacial region between cement paste and vertically cast steel at four ages in a concrete with a *w/c* ratio of 0.70: (a) calcium hydroxide, (b) porosity, (c) unreacted clinker phases, and (d) undesignated hydration products (mainly C–S–H).

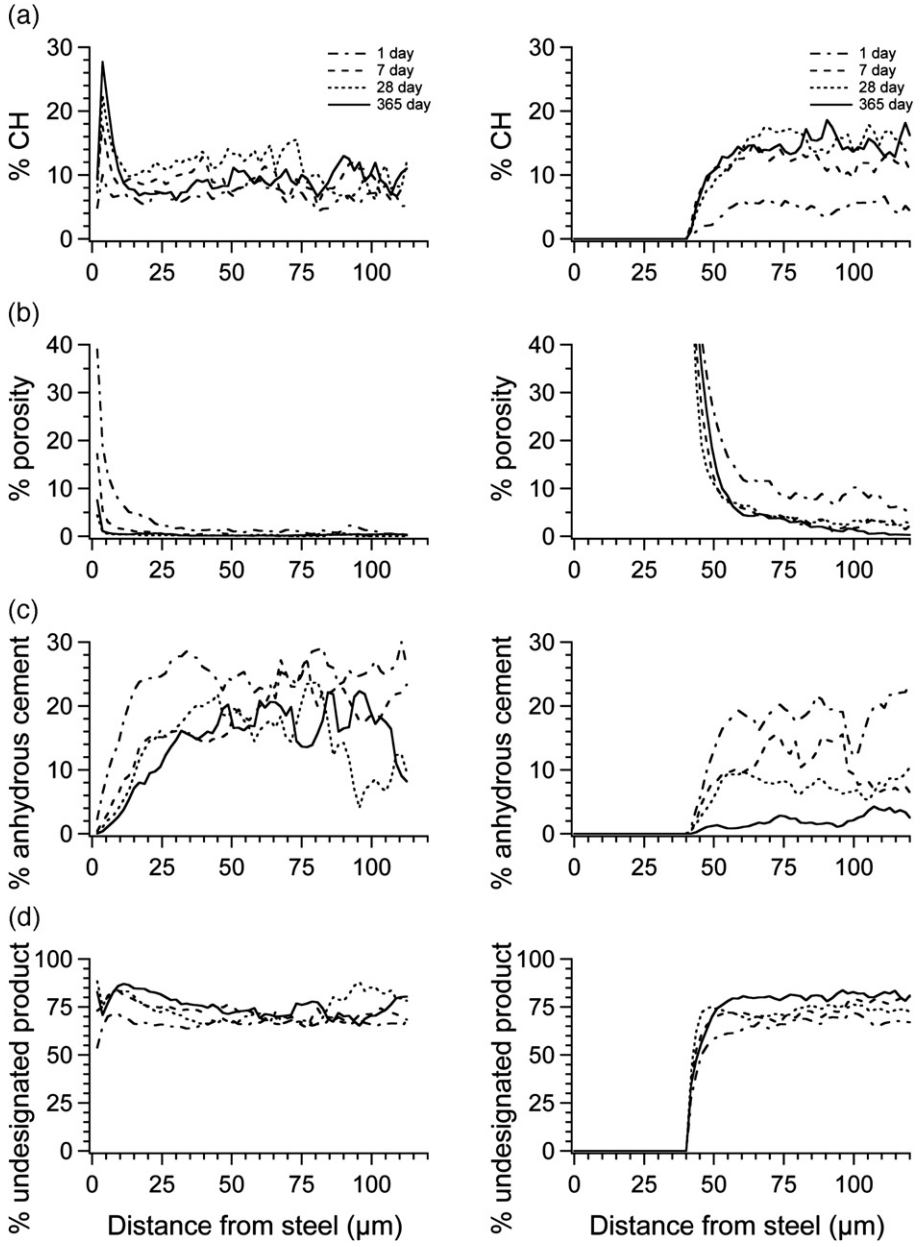

Fig. 7. Microstructural gradients in the interfacial region between cement paste and the topside (left) and underside (right) of horizontally cast steel at four ages in a concrete with a *w*/*c* ratio of 0.49: (a) calcium hydroxide, (b) porosity, (c) unreacted clinker phases, and (d) undesignated hydration products (mainly C–S–H).

similar microstructure to the lower *w*/*c* ratio mix but there is a larger bleed-water zone under the steel, which is approximately 150 μm wide and contains few hydration products. In addition, higher levels of porosity are observed within the region of paste adjacent to the bleed-water zone when compared to lower *w*/*c* ratio mixes. Very low levels of unreacted cement are present under the bar due to increased water availability, and the CH level beyond the bleed-water zone is – in contrast to the lower *w*/*c* ratio – comparable to that in the bulk paste above the bar. The high degrees of reaction under the bars in the two systems but very different quantities of CH would seem to suggest that the C–S–H in the two cases must have different Ca/Si ratios, but this was not measured and must await further work.

3.4. Effect of removing rust and mill scale

The rust and mill scale found on the bars were removed before casting vertically into one set of samples with a 0.49 *w*/*c* ratio. The resulting phase-distribution profiles are shown in Fig. 10, which should be compared with those for the uncleaned bars in Fig. 5. Two-sample *t*-tests were used to determine if there was any statistically significant effect on the CH distribution of removing the rust and mill scale, with the results for the samples hydrated for 28 and 365 days shown in Figs. 11 and 12 respectively; data for the steel–cement paste interface are given on the left of the figures, and those for the aggregate–cement paste interface on the right. Fig. 11 shows that there is essentially no

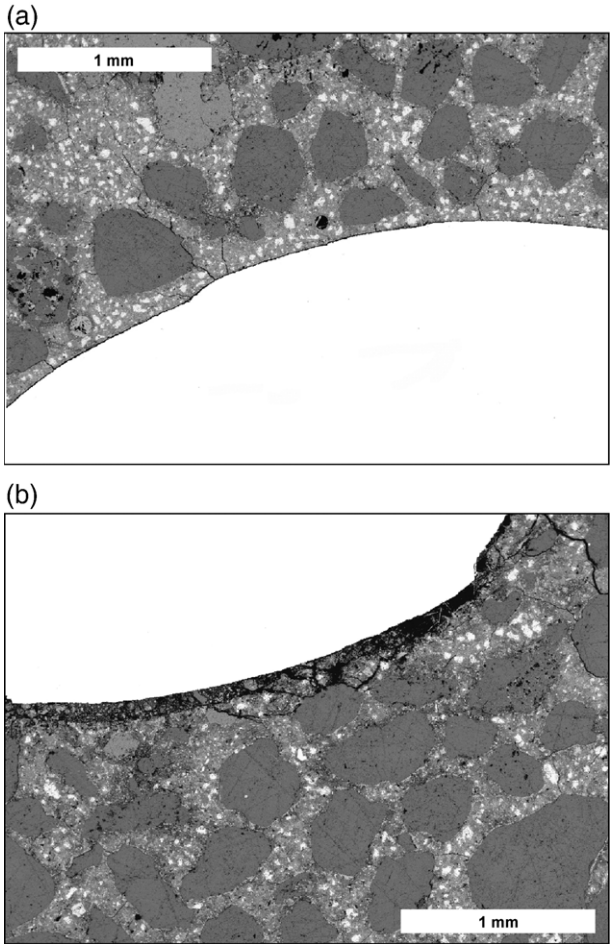

Fig. 8. Low magnification backscattered electron images illustrating the strikingly different interfaces above (top image) and below the rebar. The cracks are artefacts of specimen preparation.

difference between the distributions of CH with the cleaned or uncleaned bars at 28 days. Whilst the quantity of CH is the same in the bulk paste away from both the steel and aggregate interfaces (12%), there is clearly more CH close to the steel interface than to the aggregate. The situation is different, however, at 365 days. Whilst there is again the same amount of CH in the bulk paste (12%) and also more CH close to the steel than to the aggregate, wire-brush cleaning has had a highly significant effect on the quantity of CH close to the steel (an approximately 30% increase), which is offset by a CH-depleted region between approximately 20 and 45 μm from the interface. It is possible that crystals of CH in the region closest to the steel have become generally larger and as a consequence are more easily segmented in the BSE images. However, there does not appear to be a straightforward explanation for all the observations – which appear to require a redistribution of some CH and C–S–H – and so further investigations are necessary.

An increased amount of CH close to the steel in reinforced concrete as observed in this work may be beneficial, in that it may lead to improved local pH-buffering capacity and thus to better protection against carbonation-induced generalized corrosion; that is, it would take a longer time for the larger amount of CH near the interface to react to form calcium carbonate thus delaying the drop in pH associated with complete carbonation. However, it is possible that this potential benefit might not be realized in practice if the CH simply becomes encased in calcium carbonate whilst the surrounding C–S–H becomes completely carbonated, as has been observed in partially carbonated hardened cement pastes by transmission electron microscopy [16,17]. Certainly, a partially carbonated zone that consists of completely carbonated C–S–H and regions of CH encased in calcium carbonate would seem to be a very plausible explanation for the observation of corroded steel in regions of concrete that appears ‘uncarbonated’ to the phenolphthalein test.

4. Conclusions

A detailed and quantitative analysis of SEM BSE images has allowed statistically significant conclusions to be drawn on the phase distributions of CH, porosity, unreacted cement and C–S–H in steel– and aggregate–cement paste interfacial regions in steel reinforced concrete. The main conclusions are as follows:

(1) A larger amount of calcium hydroxide was observed close to both the steel– (30%) and aggregate– (20–25%) cement paste interfaces in reinforced concrete with vertically cast rebar when compared to the bulk cement paste (12%). At later ages the extra CH close to the interface is offset by a reduced amount of C–S–H.
(2) Increased levels of porosity and decreased levels of anhydrous cement and C–S–H were found close to both the steel– and aggregate–cement paste interfaces in reinforced concrete with vertically cast rebar when compared to the bulk cement paste.
(3) The amount of calcium hydroxide close to the steel–cement paste interface decreased as the *w*/*c* ratio increased, from around 30% at a *w*/*c* ratio of 0.49 to 19% at a *w*/*c* ratio of 0.7.
(4) The orientation of the reinforcing bars made a big difference to the composition of the steel–cement paste interface. The collection of bleed-water under the bars caused a reduction in CH content and an increase in porosity.
(5) The microstructure of the interfaces continued to change up to 365 days in some of the systems; it was generally unchanged after 28 days. This depended on the local availability of both water and space in the interfacial region.
(6) The interface around the vertically cast reinforcing bars was affected by the ribs, with the underside of the ribs having a coarser microstructure.
(7) Wire-brush cleaning of the reinforcing bars led to an approximately 30% increase in the amount of CH close to the steel relative to rusted bars at 365 days hydration, which was offset by a region that was depleted in CH between approximately 20 and 45 μm from the interface.
(8) It is possible that an increased amount of CH close to the steel in reinforced concrete may be beneficial, in that it

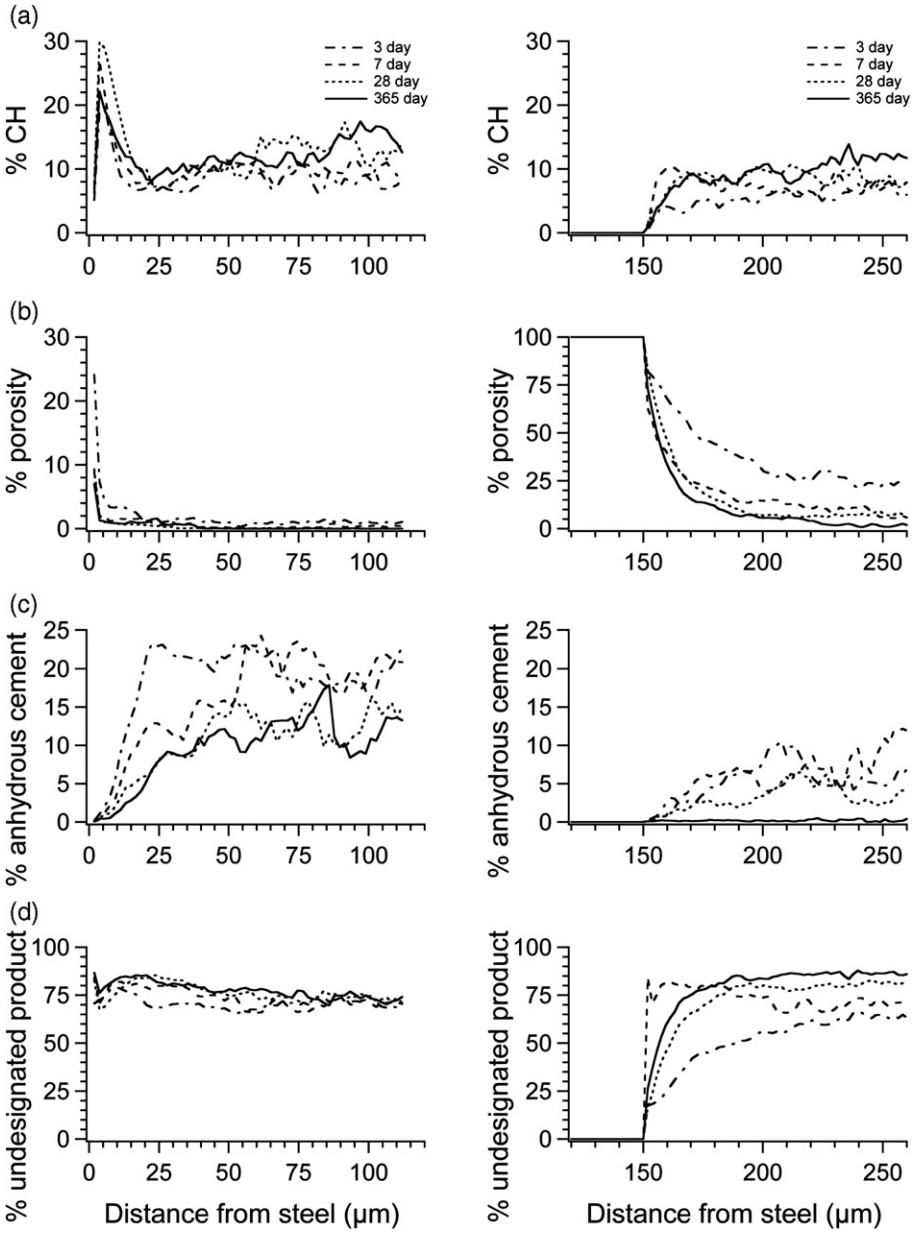

Fig. 9. Microstructural gradients in the interfacial region between cement paste and the topside (left) and underside (right) of horizontally cast steel at four ages in a concrete with a *w/c* ratio of 0.70: (a) calcium hydroxide, (b) porosity, (c) unreacted clinker phases, and (d) undesignated hydration products (mainly C–S–H).

may lead to improved local pH-buffering capacity and thus to better protection against carbonation-induced generalized corrosion; that is, it would take a longer time for the larger amount of CH near the interface to react to form calcium carbonate thus delaying the drop in pH associated with complete carbonation. However, it is possible that this potential benefit might not be realized in practice if the CH simply becomes encased in calcium carbonate whilst the surrounding C–S–H becomes completely carbonated.

Acknowledgements

Thanks are due to the EPSRC for a DTA award (ATH), to Dr Adrian Brough for valuable discussions and to Mr Saiful Duraman for processing the image in Fig. 1(a) to produce Fig. 1(f) to (h).

References

[1] M. Pourbaix, Applications of electrochemistry in corrosion science and in practice, Corr. Sci. 14 (1974) 25–83.
[2] J.G. Cabrera, Deterioration of concrete due to reinforcement steel corrosion, Cem. Concr. Compos. 18 (1996) 47–59.
[3] C.L. Page, Mechanism of corrosion protection in reinforced concrete marine structures, Nature 258 (1975) 514–515.
[4] M.N. Al Khalaf, C.L. Page, Steel/mortar interfaces: microstructural features and modes of failure, Cem. Concr. Res. 9 (1979) 197–208.
[5] L. Yue, H. Shuguang, The microstructure of the interfacial transition zone between steel and cement paste, Cem. Concr. Res. 31 (2001) 385–388.
[6] M. Moreau, Contribution to the study of adhesion between the hydrated constituents of artificial Portland cement and embedded steel, Revenue mater. 674 (1973) 4–17.

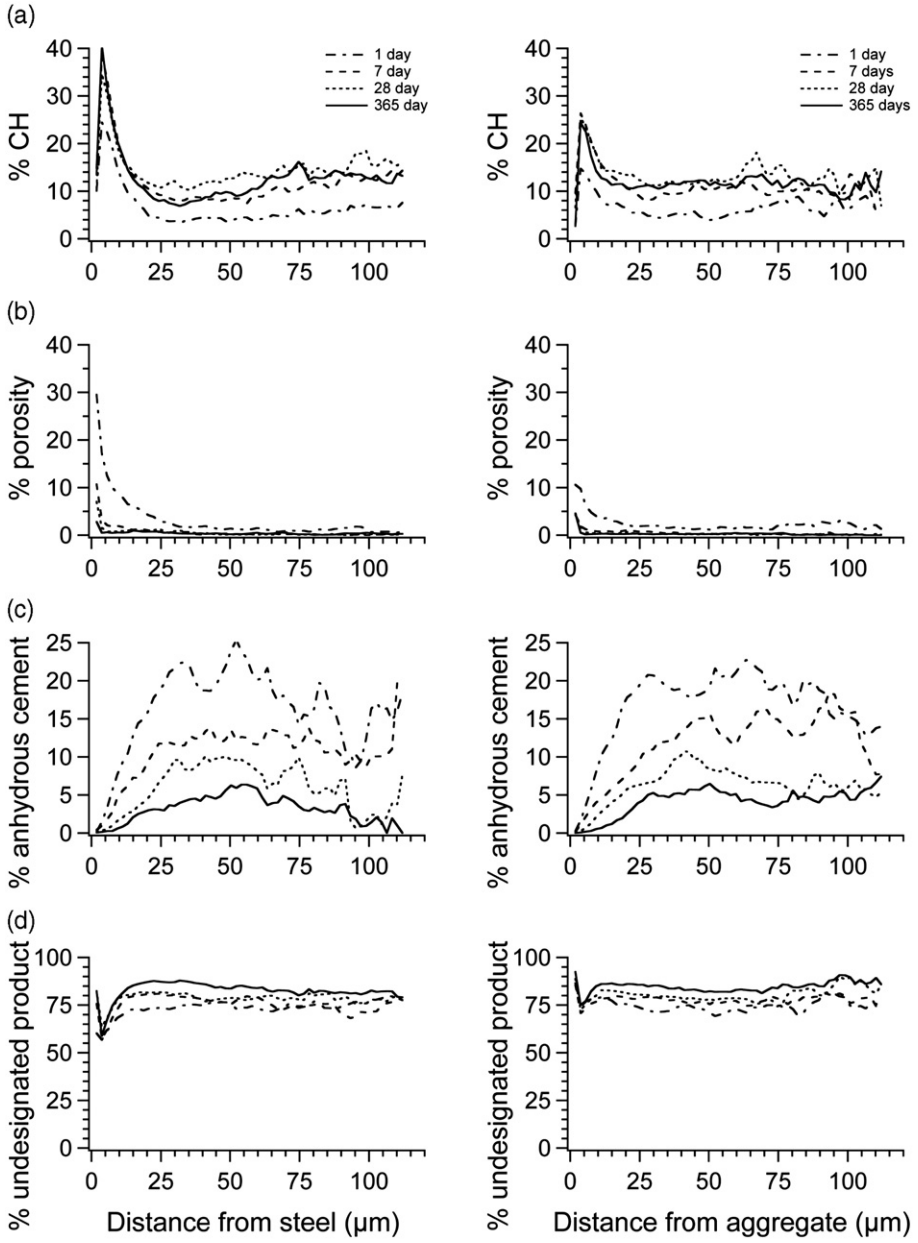

Fig. 10. Microstructural gradients in the interfacial region between cement paste and vertically cast steel (left) and aggregate (right) at four ages in a concrete with a *w/c* ratio of 0.49: (a) calcium hydroxide, (b) porosity, (c) unreacted clinker phases, and (d) undesignated hydration products (mainly C–S–H). The steel had been wire-brush cleaned before casting.

[7] K.K. Sagoe-Crentsil, F.P. Glasser, Analysis of the steel–concrete interface, in: C.L. Page, K.W.J. Treadaway, P.B. Bamforth (Eds.), Corrosion of Reinforcement in Concrete, Elsevier, 1990, pp. 74–86.

[8] G.K. Glass, R. Yang, T. Dickhaus, N.R. Buenfeld, Backscattered electron imaging of the steel concrete interface, Corr. Sci. 43 (2001) 605–610.

[9] A.M. Zayed, The nature of the concrete–steel rebar interface in plain and silica fume concrete, in: F.P. Glasser, G.J. McCarthy, J.F. Young, T.O. Mason, P.L. Pratt (Eds.), Advanced Cementitious Systems: Mechanisms and Properties, Mater. Res. Soc. Symp. Proc., vol. 245, 1992, pp. 341–347, Pittsburgh, PA.

[10] A.M. Zayed, A. Slater-Haase, The nature of the concrete–steel rebar interface and its effects on corrosion, Corrosion92, National Association of Corrosion Engineers Annual Conference, Nashville TN, 1992, pp. 209/2–209/10.

[11] M.K. Head, Influence of the interfacial zone (ITZ) on the properties of concrete, PhD Thesis, University of Leeds, School of Civil Engineering, 2001.

[12] I.G. Richardson, Electron microscopy of cements, in: J. Bensted, P. Barnes (Eds.), Structure and Performance of Cements, 2nd ed., Spon Press, London, 2002, pp. 500–556.

[13] K.L. Scrivener, H.H. Patel, P.L. Pratt, L.J. Parrot, Analysis of phases in cement paste using backscattered electron images, methanol absorption and thermogravimetric analysis, in: L.J. Struble, P.W. Brown (Eds.), Microstructural Development During Hydration of Cement, Mater. Res. Soc. Symp. Proc., vol. 85, 1987, pp. 67–76, Pittsburgh, PA.

[14] K.L. Scrivener, Backscattered electron imaging of cementitious microstructures: understanding and quantification, Cem. Concr. Compos. 26 (2004) 935–945.

[15] K.L. Scrivener, A.K. Crumbie, P. Laugesen, The interfacial transition zone (ITZ) between cement paste and aggregate in concrete, Interface Sci. 12 (2004) 411–421.

[16] G.W. Groves, D.I. Rodway, I.G. Richardson, The carbonation of hardened cement pastes, Adv. Cem. Res. 3 (1990) 117–125.

[17] G.W. Groves, A.R. Brough, I.G. Richardson, C.M. Dobson, Progressive changes in the structure of hardened C_3S pastes due to carbonation, J. Am. Ceram. Soc. 74 (1991) 2891–2896.

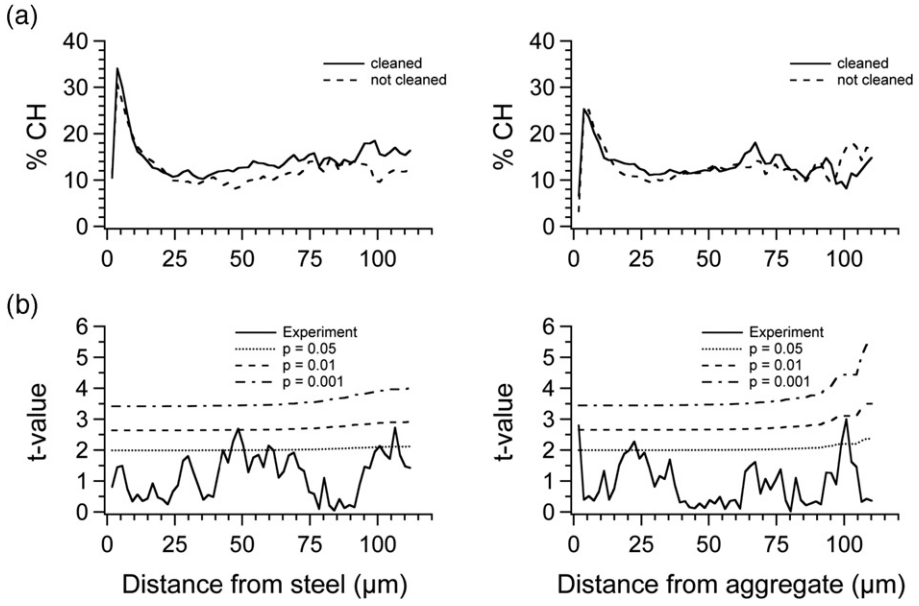

Fig. 11. (a) The distribution of CH in the interfacial regions between cement paste and vertically cast steel (left) and aggregate (right) in concretes where the steel was rusty or wire-brush cleaned (*w/c* ratio of 0.49 hydrated for 28 days). (b) The results of two-sample *t*-tests comparing the mean CH values at 1.86 μm increments from the interfaces; two-tailed critical *t*-curves are given for probabilities of 95, 99 and 99.9%, which are by convention commonly referred to respectively as statistically 'significant', 'highly significant', and 'very highly significant' threshold values (so for example, the result would be considered statistically significant if the calculated *t*-value was greater than the critical *t*-curve for 95% probability ($p = 0.05$)).

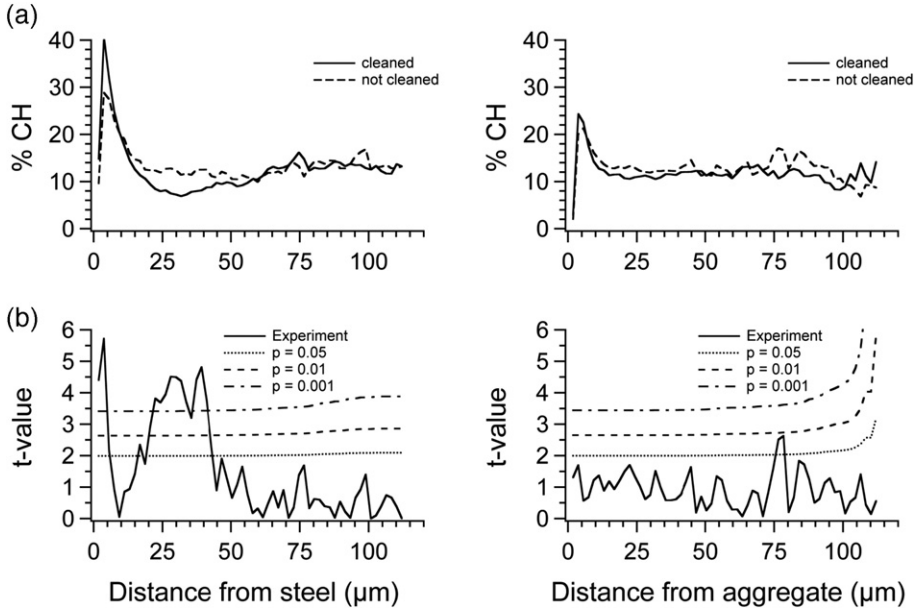

Fig. 12. As Fig. 11 but hydrated for 365 days.